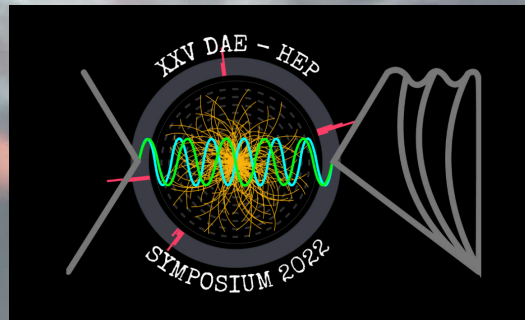


# Investigating Lorentz Invariance Violation with the long-baseline experiment P<sub>2</sub>O



Nishat Fiza  
IISER Mohali, India



XXV<sup>th</sup> DAE BRNS Symposium 2022  
December 15<sup>th</sup>, 2022



# Plan of the talk:

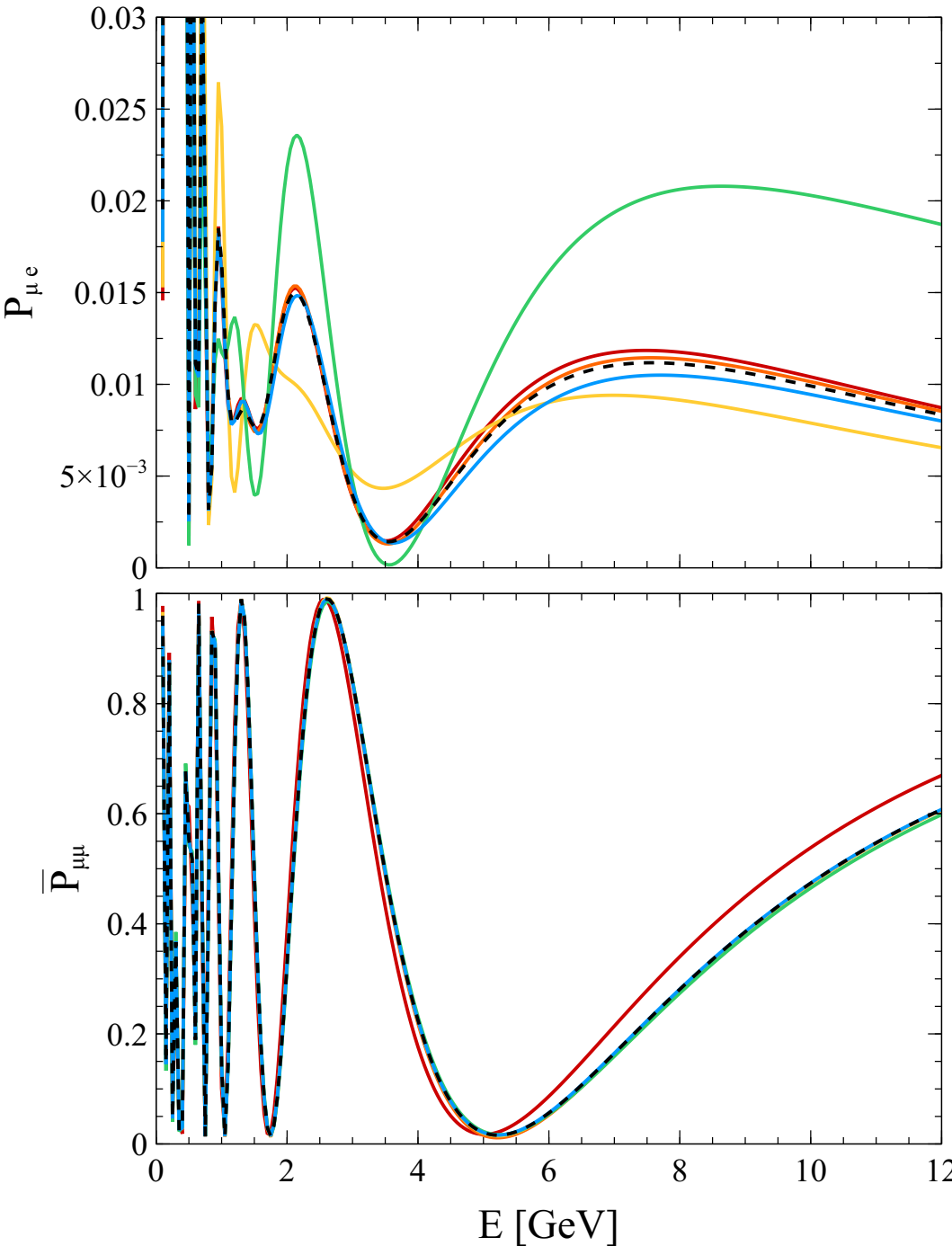
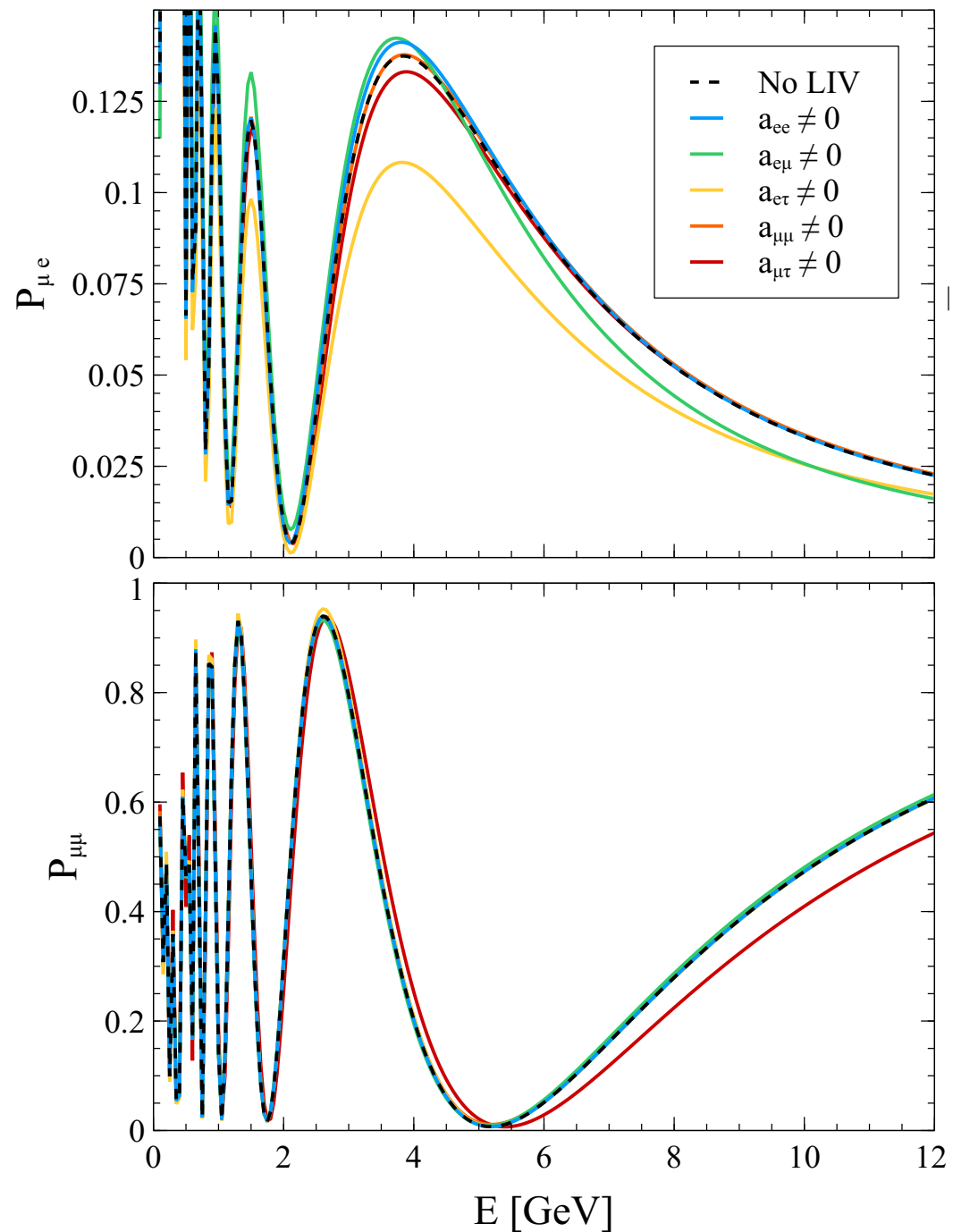
- Introduction
- Effect of LIV at probability level
- Correlation of LIV parameters with the oscillation parameters
- Bounds on the LIV parameters
- Summary

# Lorentz Invariance Violation:

- CPT violation can be probed through Lorentz invariance violation
- Spontaneous breakdown of Lorentz invariance may occur at Planck scale ( $M_P \sim 10^{19} GeV$ )
- At low energy, LBL  $\nu$  oscillation experiments can probe LIV
- Lagrangian in presence of LIV:  $\mathcal{L} = \frac{1}{2}\bar{\Psi} \left( i\gamma^\mu \partial_\mu - M + \hat{\mathcal{Q}} \right) \Psi + \text{h.c.}$ <sup>[1]</sup>
- $\mathcal{L}_{\text{LIV}} \supset -\frac{1}{2} \left[ a_{\alpha\beta}^\mu \bar{\Psi}_\alpha \gamma_\mu \Psi_\beta + b_{\alpha\beta}^\mu \bar{\Psi}_\alpha \gamma_5 \gamma_\mu \right] ; \quad (a_L)_{\alpha\beta}^\mu = (a + b)_{\alpha\beta}^\mu$
- Effective Hamiltonian:  $H \simeq \frac{1}{2E} U \begin{pmatrix} m_1^2 & 0 & 0 \\ 0 & m_2^2 & 0 \\ 0 & 0 & m_3^2 \end{pmatrix} U^\dagger + \sqrt{2} G_F N_e \begin{pmatrix} 1 & 0 & 0 \\ 0 & 0 & 0 \\ 0 & 0 & 0 \end{pmatrix} + \begin{pmatrix} a_{ee} & a_{e\mu} & a_{e\tau} \\ a_{e\mu}^* & a_{\mu\mu} & a_{\mu\tau} \\ a_{e\tau}^* & a_{\mu\tau}^* & a_{\tau\tau} \end{pmatrix}$

[1] Kostelecky, Mewes: arXiv:1112.6395

# How do LIV parameters change the probability?



P2O experiment

Baseline 2595 km<sup>[2]</sup>

$$a_{\alpha\beta} = 5 \times 10^{-23} \text{ GeV} \text{ where } \alpha, \beta = e, \mu, \tau$$

# How do LIV parameters change the probability?

$$P_{\mu e}(SI + LIV) \simeq P_{\mu e}(SI, a_{ee}) + P_{\mu e}(|a_{e\mu}|) + P_{\mu e}(|a_{e\tau}|)$$

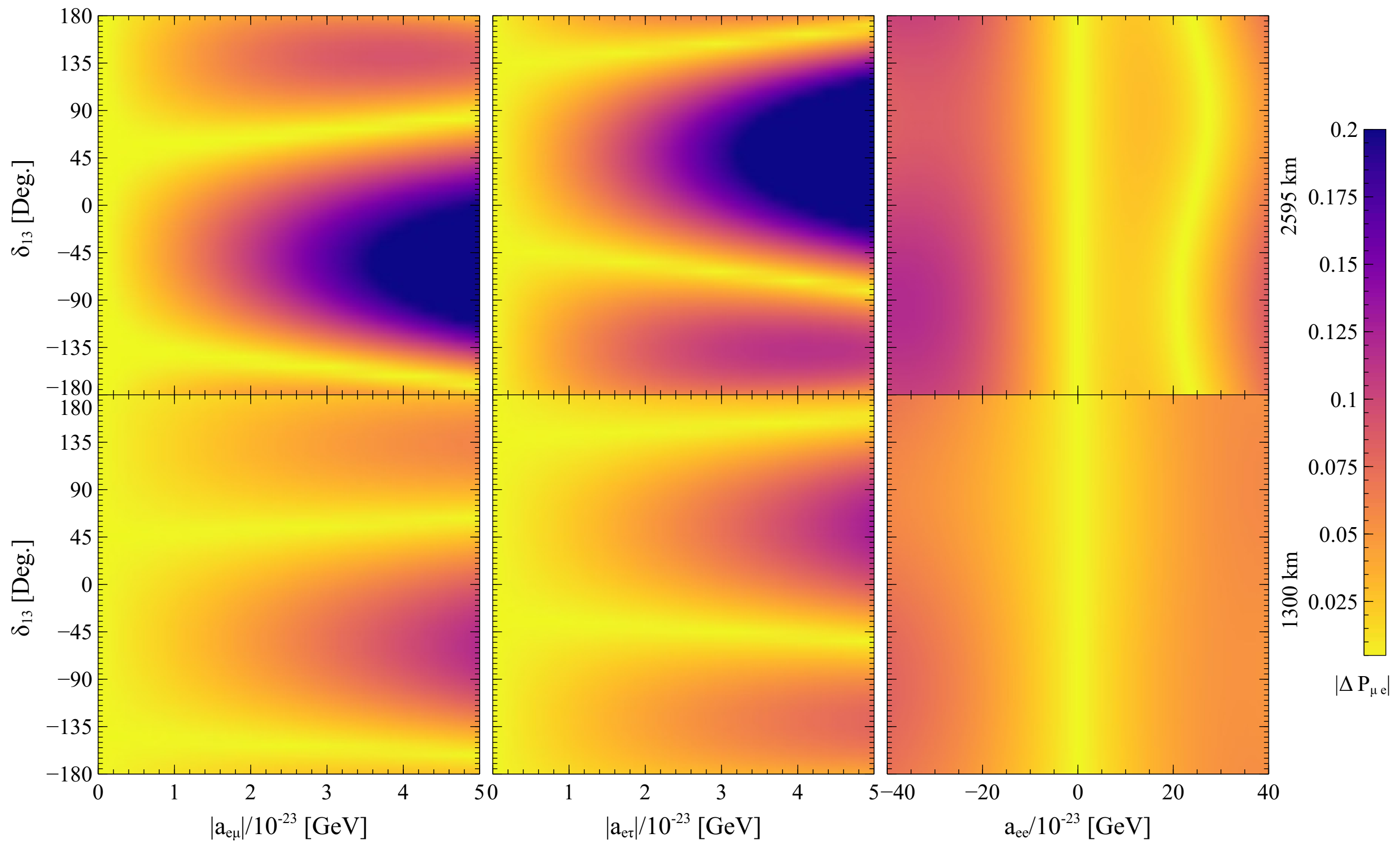
The diagram illustrates the decomposition of the total probability. A horizontal line with a bracket spans the terms  $P_{\mu e}(|a_{e\mu}|)$  and  $P_{\mu e}(|a_{e\tau}|)$ . Two arrows point downwards from this bracket to two text boxes. The left arrow points to the text 'Combination of standard CC interaction between  $\nu_e$  and e in earth's matter and  $a_{ee}$ '. The right arrow points to the text 'Deviation in the probability due to  $|a_{e\mu}|$  and  $|a_{e\tau}|$ '.

Combination of standard CC interaction between  $\nu_e$  and e in earth's matter and  $a_{ee}$

Deviation in the probability due to  $|a_{e\mu}|$  and  $|a_{e\tau}|$

$$|\Delta P_{\mu e}| = |P_{\mu e}(SI + LIV) - P_{\mu e}(SI)|$$

# Heatplot for $|\Delta P_{\mu e}|$



$|\Delta P_{\mu e}|$  for **P2O** and **DUNE** plotted at **5 GeV** and **2.5 GeV** respectively

# Heatplot for $|\Delta P_{\mu e}|$

$$\Delta P_{\mu e}(|a_{e\mu}|) \simeq 8 |a_{e\mu}| \frac{\pi}{2} E s_{13} \sin 2\theta_{23} c_{23} \left[ -\sin \delta_{13} + \frac{2}{\pi} \frac{s_{23}^2}{c_{23}^2} \cos \delta_{13} \right]$$

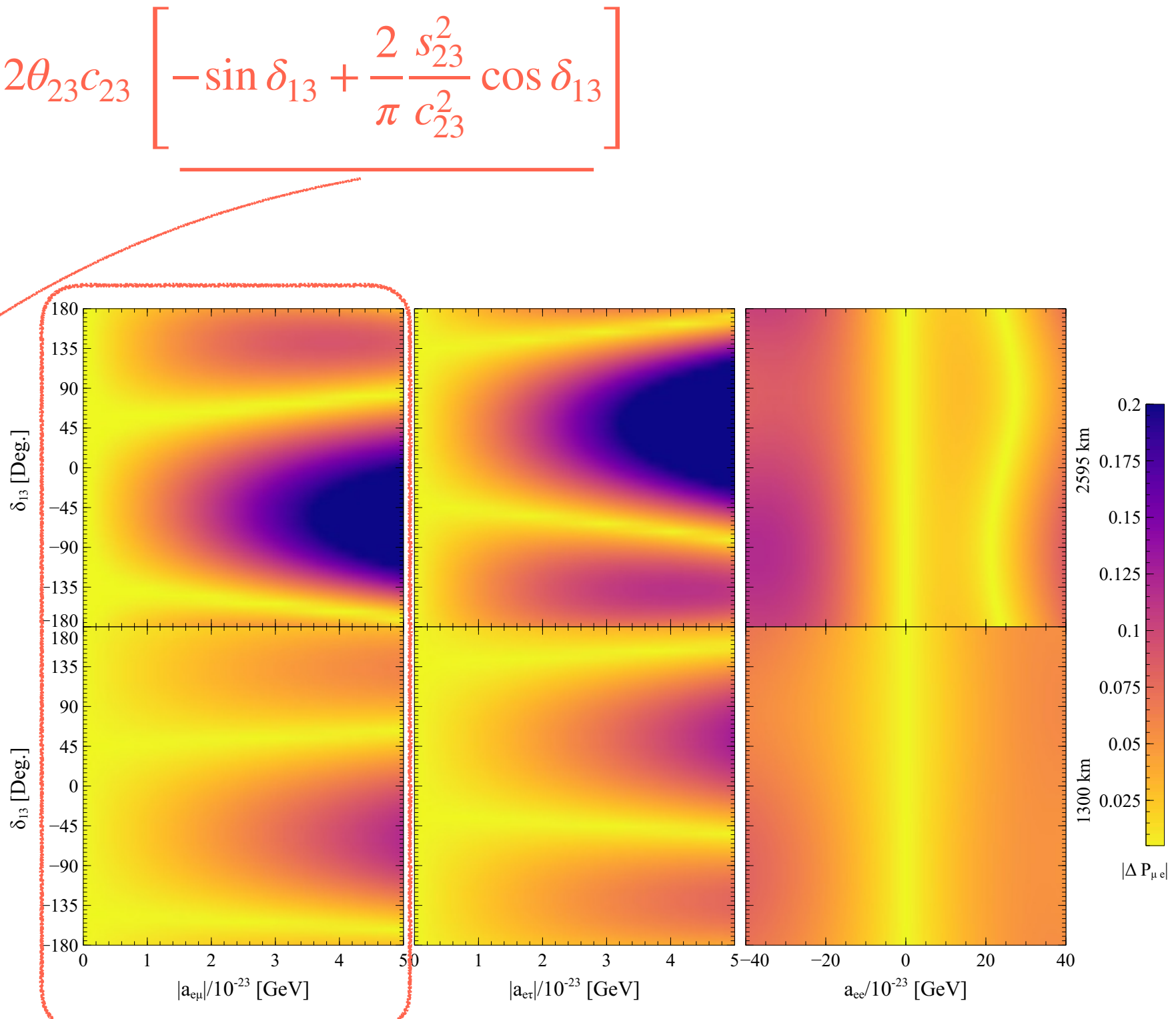
$\Delta P(|a_{e\mu}|) \simeq 0$ ; if we have:

$$|a_{e\mu}| = 0$$

Or

$$\tan \delta_{13} = \frac{2}{\pi} \frac{s_{23}^2}{c_{23}^2}$$

which gives:  
 $\delta_{13} = 39^\circ, -141^\circ$



# Heatplot for $|\Delta P_{\mu e}|$

$$\Delta P_{\mu e}(|a_{e\tau}|) \simeq 8 |a_{e\tau}| \frac{\pi}{2} E s_{13} \sin 2\theta_{23} c_{23} \left[ -\sin \delta_{13} + \frac{2}{\pi} \cos \delta_{13} \right]$$

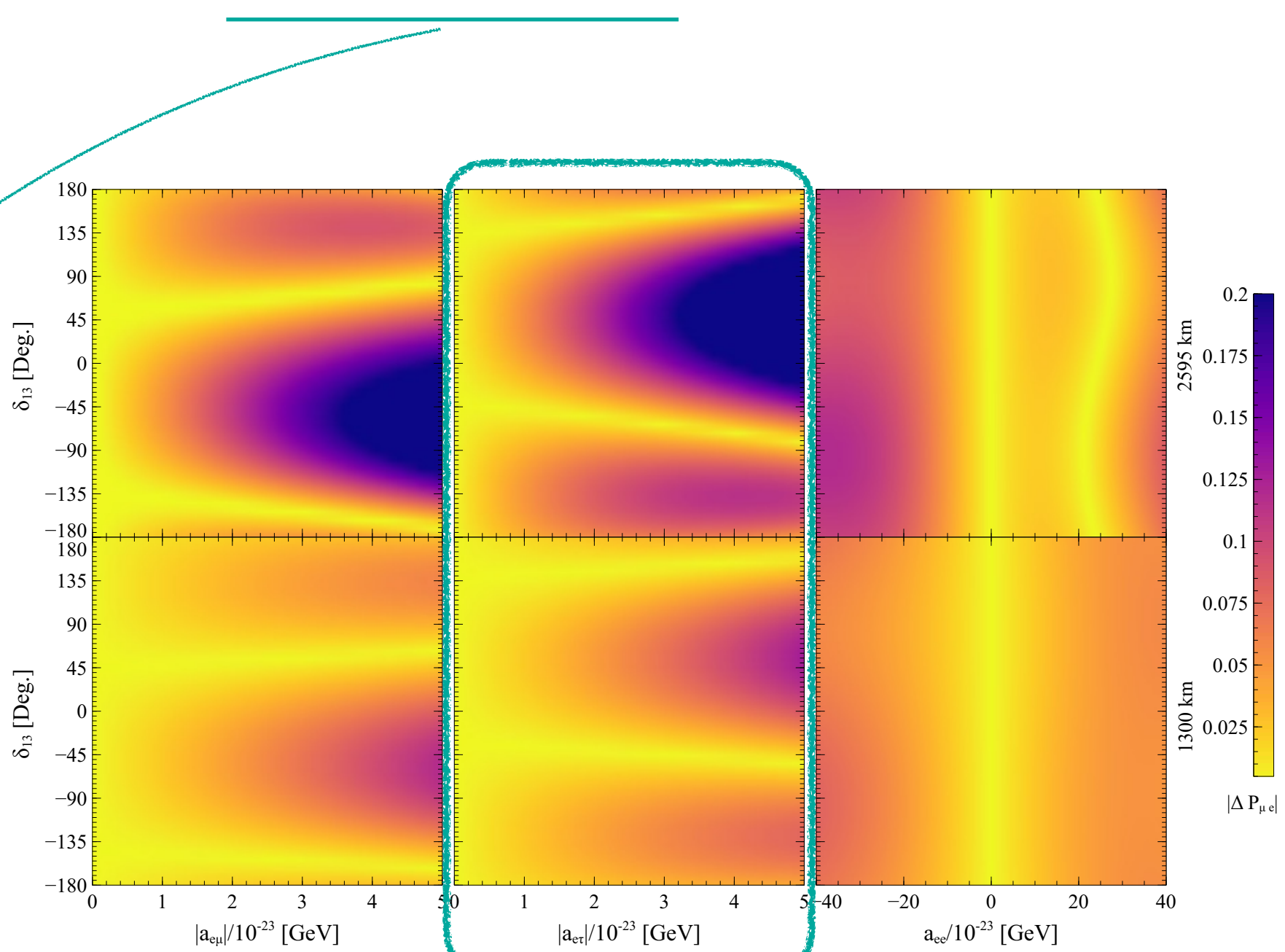
$\Delta P(|a_{e\tau}|) \simeq 0$ ; if we have:

$$|a_{e\tau}| = 0$$

Or

$$\tan \delta_{13} = \frac{2}{\pi}$$

which gives:  
 $\delta_{13} = -33^\circ, 147^\circ$



# Heatplot for $|\Delta P_{\mu e}|$

$$\left[ \underbrace{\frac{\sin[1 - \hat{A}(1 + \hat{a}_{ee})]\Delta}{1 - \hat{A}(1 + \hat{a}_{ee})}}_{I_-} - \underbrace{\frac{\sin[1 - \hat{A}]\Delta}{1 - \hat{A}} \right] \times \left[ \underbrace{\frac{\sin[1 - \hat{A}(1 + \hat{a}_{ee})]\Delta}{1 - \hat{A}(1 + \hat{a}_{ee})}}_{I_+} + \underbrace{\frac{\sin[1 - \hat{A}]\Delta}{1 - \hat{A}} \right] = 0$$

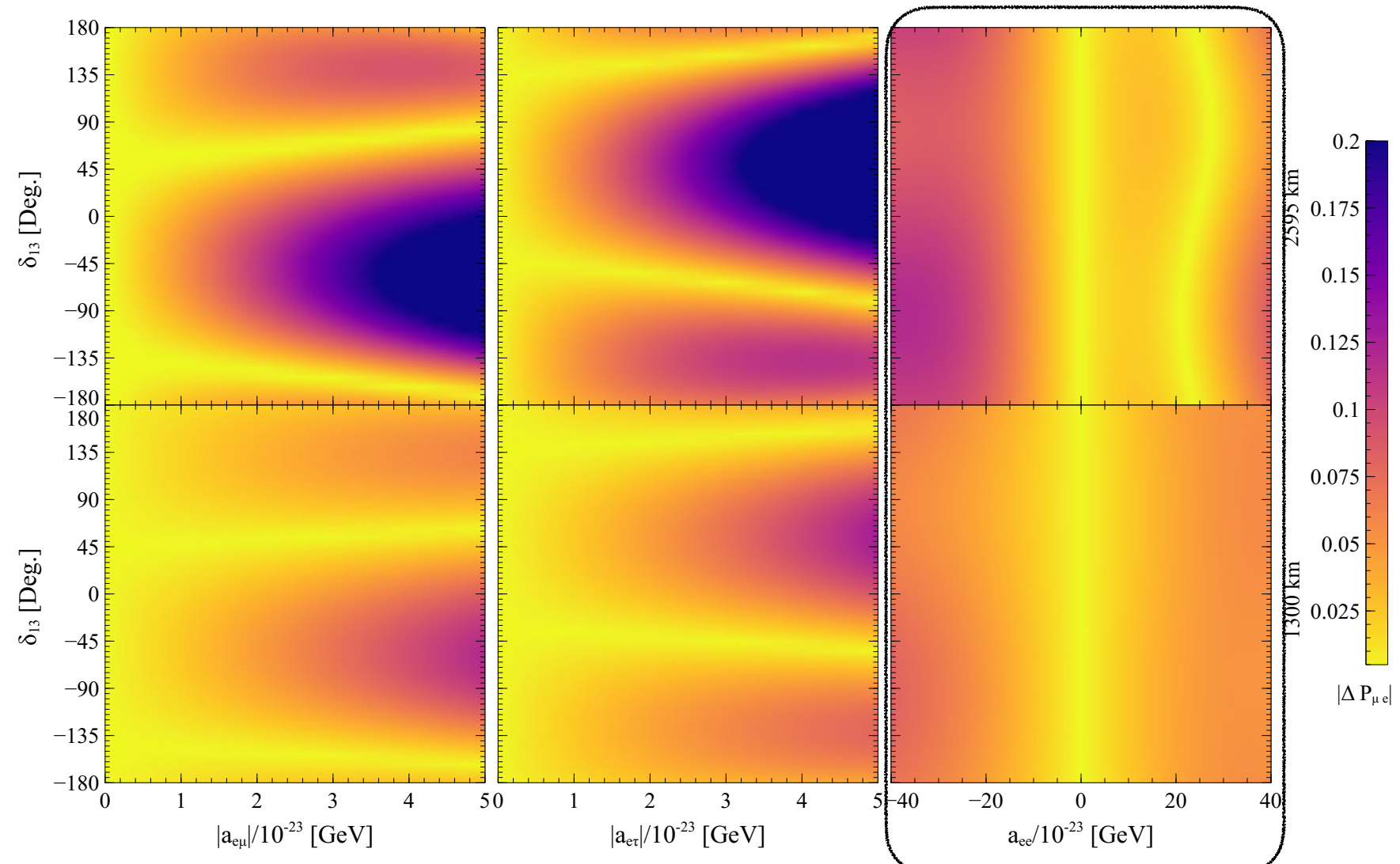
$I_-$                                      $I_+$

$a_{ee} \simeq 24.8 \times 10^{-23} \text{ GeV}$

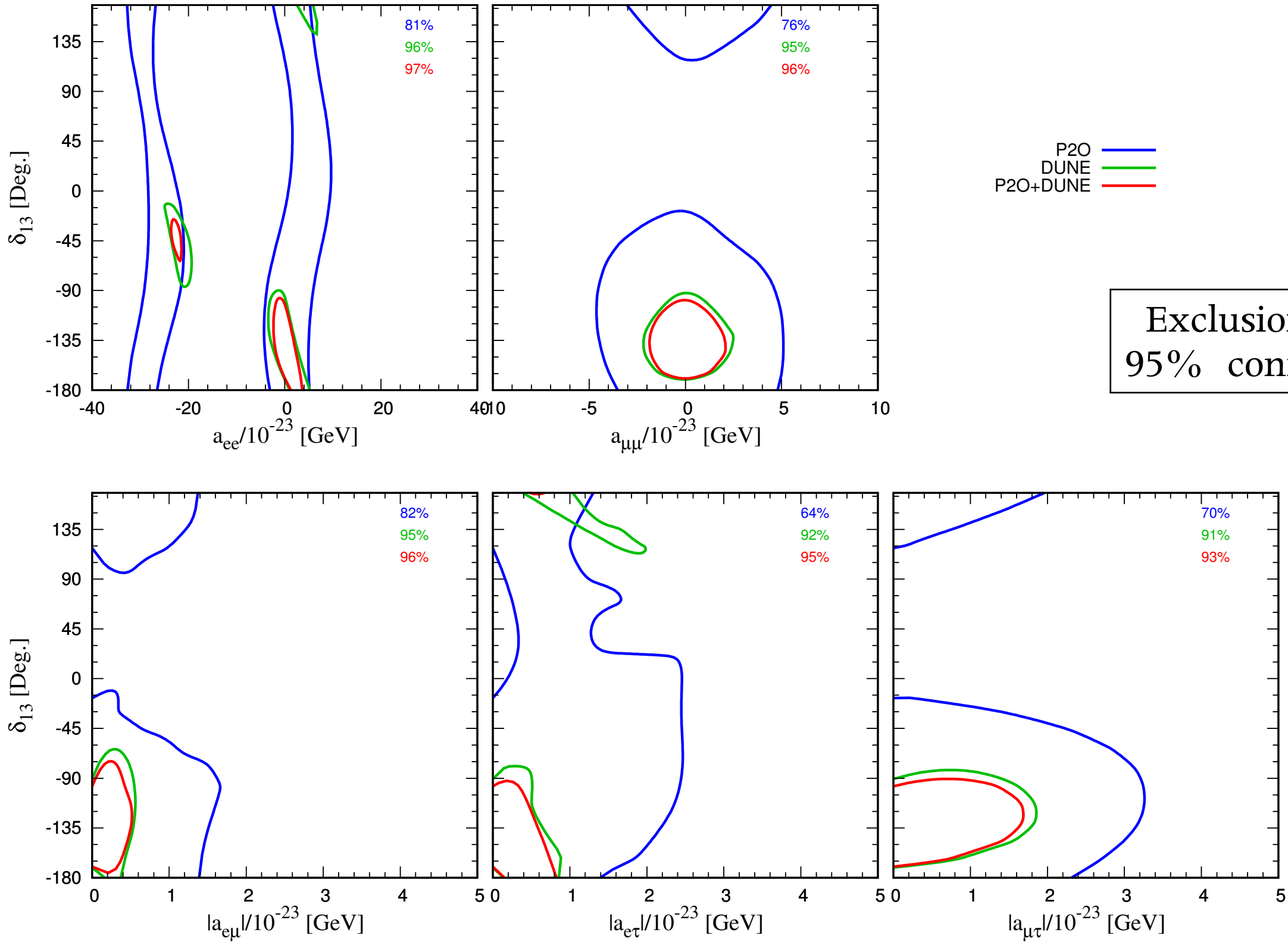
where,  $\Delta = \frac{\Delta m_{31}^2 L}{4E}$

$$\hat{A} = \frac{2\sqrt{2}G_F N_e E}{\Delta m_{31}^2}$$

$$\hat{a}_{ee} = \frac{a_{ee}}{\sqrt{2}G_F N_e}$$

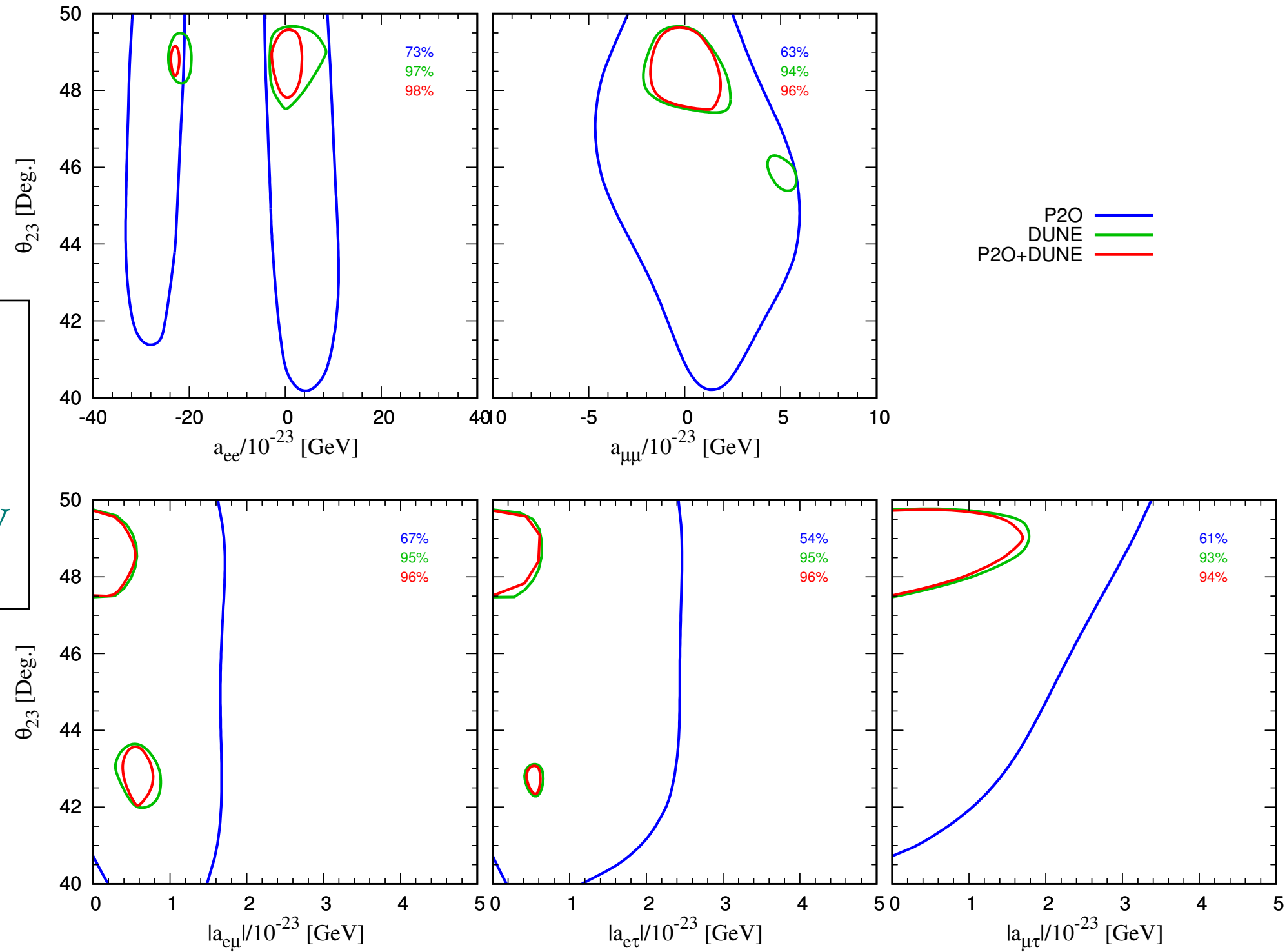


# Exclusion region in correlation with $\delta_{13}$



# Exclusion region in correlation with $\theta_{23}$

Combining the simulated data for DUNE and P<sub>2</sub>O lifts the octant degeneracy in case of  $\theta_{23}$



# Degenerate region in correlation to $a_{ee}$

$$\Delta\chi^2(a_{ee}) \sim \Delta P_{\mu e}(a_{ee})$$

$$\sim \left[ \frac{\sin[1 - \hat{A}(1 + \hat{a}_{ee})]\Delta}{1 - \hat{A}(1 + \hat{a}_{ee})} - \frac{\sin[1 - \hat{A}]\Delta}{1 - \hat{A}} \right] \times \left[ \frac{\sin[1 - \hat{A}(1 + \hat{a}_{ee})]\Delta}{1 - \hat{A}(1 + \hat{a}_{ee})} + \frac{\sin[1 - \hat{A}]\Delta}{1 - \hat{A}} \right]$$

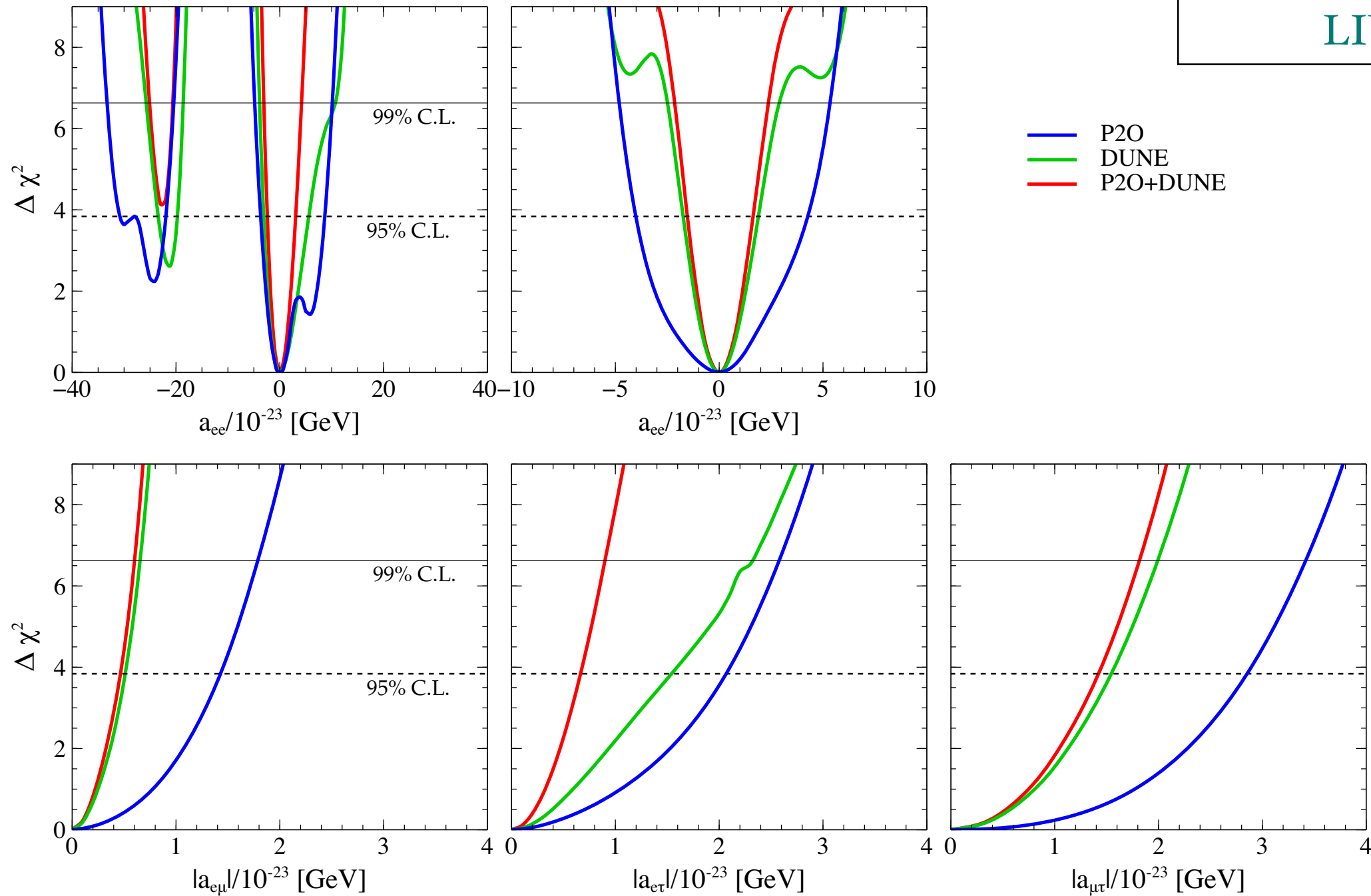
- Marginalization over the mass hierarchy
- For inverted hierarchy,  $\hat{A}$  and  $\Delta$  changes sign

where,  $\Delta = \frac{\Delta m_{31}^2 L}{4E}$   
 $\hat{A} = \frac{2\sqrt{2}G_F N_e E}{\Delta m_{31}^2}$

$$\Delta\chi^2 \sim \left[ \underbrace{\frac{\sin[1 + \hat{A}(1 + \hat{a}_{ee})]\Delta}{1 + \hat{A}(1 + \hat{a}_{ee})} + \frac{\sin[1 - \hat{A}]\Delta}{1 - \hat{A}}}_{a_{ee} = 0} \right] \times \left[ \underbrace{\frac{\sin[1 + \hat{A}(1 + \hat{a}_{ee})]\Delta}{1 + \hat{A}(1 + \hat{a}_{ee})} - \frac{\sin[1 - \hat{A}]\Delta}{1 - \hat{A}}}_{a_{ee} \simeq -22 \times 10^{-23} \text{ GeV}} \right]$$

# Results:

Expected sensitivity of DUNE  
and P2O experiment to the  
LIV parameters



# Bounds on the LIV parameters

(At 95% confidence level)

Parameter	Bounds from DUNE [ $10^{-23}$ GeV]	Bounds from P2O [ $10^{-23}$ GeV]	Bounds from (P2O+DUNE) [ $10^{-23}$ GeV]
$a_{ee}$	$[-24 < a_{ee} < -20]$ $\cup [-3.2 < a_{ee} < 5.6]$	$[-30.8 < a_{ee} < -21.9]$ $\cup [-3.9 < a_{ee} < 8.6]$	$-2.6 < a_{ee} < 3.3$
$a_{\mu\mu}$	$-1.9 < a_{\mu\mu} < 2.0$	$-4.0 < a_{\mu\mu} < 4.3$	$-1.6 < a_{\mu\mu} < 1.6$
$ a_{e\mu} $	0.6	1.6	0.4
$ a_{e\tau} $	1.3	2.1	0.7
$ a_{\mu\tau} $	1.5	2.9	1.3

# Summary

- We consider P2O to study LIV
- Effect of LIV on probability
- Effect of LIV parameters on  $|\Delta P_{\alpha\beta}|$
- $\Delta\chi^2$  analysis of LIV parameters in correlation to standard oscillation parameters
- Bounds on the LIV parameters



# Back-up

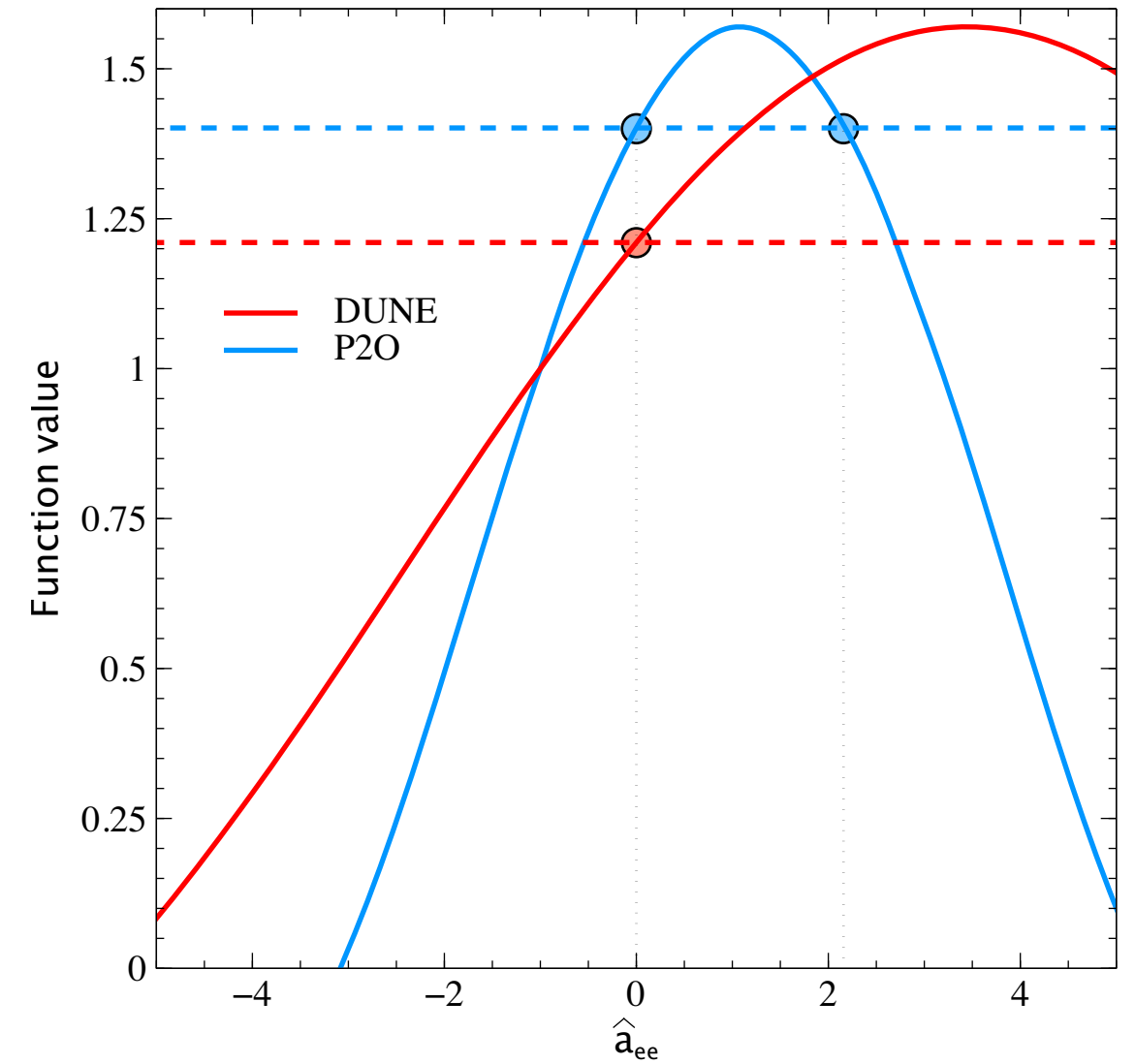
$$I_- = \left[ \frac{\sin[1 - \hat{A}(1 + \hat{a}_{ee})]\Delta}{1 - \hat{A}(1 + \hat{a}_{ee})} - \frac{\sin[1 - \hat{A}]\Delta}{1 - \hat{A}} \right]$$

$$\hat{A} = \frac{2\sqrt{2}G_F N_e E}{\Delta m_{31}^2}$$

$$\approx 0.03 \times \rho [g/cm^3] \times E [GeV]$$

$$\approx 0.225 \text{ for DUNE } [\rho = 3, E = 2.5]$$

$$\approx 0.448 \text{ for P2O } [\rho = 3.2, E = 5]$$



The two terms in  $I_-$  are plotted for both DUNE (red) and P2O (blue) as functions of the parameter  $\hat{a}_{ee} = a_{ee}\sqrt{2}G_F N_e$ . The solid curve is the first term ( $\frac{\sin[1 - \hat{A}(1 + \hat{a}_{ee})]\Delta}{1 - \hat{A}(1 + \hat{a}_{ee})}$ ), while the dashed curve is the second term ( $\frac{\sin[1 - \hat{A}]\Delta}{1 - \hat{A}}$ ). The small coloured circles show the locations of solutions where the two terms intersect.

# Back-up

